Review

Journal of
Nanoscience and Nanotechnology
Vol. 14, 1120–1133, 2014
www.aspbs.com/jnn

Graphene Doping Methods and Device Applications

Jong Sik Oh[1], Kyong Nam Kim[1], and Geun Young Yeom[1, 2, *]

[1] *Department of Advanced Materials Engineering, Sungkyunkwan University, Suwon, Gyeonggi-do 440-746, South Korea*
[2] *SKKU Advanced Institute of Nano Technology (SAINT), Sungkyunkwan University, Suwon, Gyeonggi-do 440-746, South Korea*

Graphene has recently been studied as a promising material to replace and enhance conventional electronic materials in various fields such as electronics, photovoltaics, sensors, etc. However, for the electronic applications of graphene prepared by various techniques such as chemical vapor deposition, chemical exfoliation, mechanical exfoliation, etc., critical limitations are found due to the defects in the graphene in addition to the absence of a semiconducting band gap. For that, many researchers have investigated the doped graphene which is effective to tailor its electronic property and chemical reactivity. This work presents a review of the various graphene doping methods and their device applications. As doping methods, direct synthesis method and post treatment method could be categorized. Because the latter case has been widely investigated and used in various electronic applications, we will focus on the post treatment method. Post treatment method could be further classified into wet and dry doping methods. In the case of wet doping, acid treatment, metal chloride, and organic material coating are the methods used to functionalize graphene by using dip-coating, spin coating, etc. Electron charge transfer achieved from graphene to dopants or from dopants to graphene makes *p*-type or *n*-type graphenes, respectively, with sheet resistance reduction effect. In the case of dry doping, it can be further categorized into electrostatic field method, evaporation method, thermal treatment method, plasma treatment method, etc. These doping techniques modify Fermi energy level of graphene and functionalize the property of graphene. Finally, some perspectives and device applications of doped graphene are also briefly discussed.

Keywords: Graphene, Doping, Wet Doping, Dry Doping, Applications, Electronic Devices.

CONTENTS

1. INTRODUCTION

Graphene consists of a single sheet of carbon atoms arranged in a honeycomb lattice and exhibits a number of fascinating properties.[1–4] Graphene possesses remarkable high thermal conductivity, high charge carrier mobility, high optical transmittance, and flexibility with strong Young's modulus.[4–6] However, tuning physicochemical properties becomes necessary[7] in many graphene applications because of intrinsic graphene properties like zero-bandgap and high sheet resistance that are not suitable to various applications due to the defects generated during the graphene fabrication using specific methods.[8, 9]

For the application of graphene in various fields, doping is one of the efficient ways because it can tailor the electrical properties of graphene. Many researchers have investigated graphene doping methods through various processes, and they could be categorized into direct synthesis method and post treatment method. The direct synthesis is the doping method where the graphene is doped during graphene growth such as chemical vapor deposition (CVD), segregation growth, solvothermal approaches, etc., and the post treatment is the doping method where the graphene

*Author to whom correspondence should be addressed.

 1533-4880/2014/14/1120/014 doi:10.1166/jnn.2014.9118

is doped after the graphene synthesis. The direct synthesis method has a potential to create a homogeneous doping over the bulk material than that of the post treatment method. However, the results reported so far were not so successful in the aspects of controllability, process time, and easiness.[10–15]

In this review, we focus on various post treatment methods for graphene doping and describe their doping effects and doping mechanisms. In addition, the applications of doped graphene on various current and possible devices are also briefly described.

2. DOPING METHODS

As mentioned above, doped graphene for various electrical properties could be obtained through the direct synthesis and the post treatment. In the case of the post treatment, it could be categorized into wet doping methods and dry doping methods, and the doping is related to the surface region of graphene, not the bulk material region. The wet doping methods can be achieved by acid treatment, metal chloride treatment, and organic material coating on the graphene surface using dip coating, spin coating, etc. In the case of dry doping, the doping is achieved by electrostatic field formation, deposition by evaporation, thermal treatment, plasma treatment, etc. These methods have merits such as controllability of dopant, scalability, and easiness over those of the direct synthesis methods.

2.1. Wet Doping

In general, the wet doping is carried out simply by spin coating or dip coating of a dopant containing solution. These doping methods are generally surface transfer doping and are also called adsorbate-induced doping. Charge transfer doping is acheived by exchanging electrons between dopants and a graphene, that is, by tranferring electrons from graphene to dopants (p-type graphene) or from dopants to graphene (n-type graphene).[16] Figure 1 shows the differences in the doping mechanism between classical doping and surface transfer doping. E_f, E_c and E_v in the figure represent Fermi energy level, conduction energy level, and valance energy level. In the surface transfer doping mechanism, the surface dopants possess

Jong Sik Oh obtained a Bachelor of electronics from Sungkyunkwan University, South Korea (2009). He is currently a Ph.D. candidate in Advanced Materials Science and Engineering at the Sungkyunkwan University with G. Y. Yeom. His research focuses on the graphene electronics and doping process.

Kyong Nam Kim received a Ph.D. degree in Advanced Materials and Engineering from Sungkyunkwan University (2007). He is currently a research associate professor in Advanced Materials and Engineering from Sungkyunkwan University. Prior to joining Sungkyunkwan University as research professor, he spent a year as a post-doctoral position in Nuclear Engineering of University of Illinois at Urbana-Champaign, Urbana. His research field is on plasma processing related to the semiconductor and flat panel display and 2D materials.

Geun Young Yeom received a Ph.D. degree in Electronic Materials Engineering from University of Illinois at Urbana-Champaign, Urbana (1989). Prior to joining Sungkyunkwan University, he was a process development position for Tektronix Inc. in Beverton, Oregon, USA. During his 2 years at Tektronix Inc. He spent time doing responsibility of developing etching processes for a bipolar IC. Also, he joined Silicon Systems Inc. for one year located at Tustin CA, USA. Currently, he is working on various plasma processing technologies and 2D materials research.

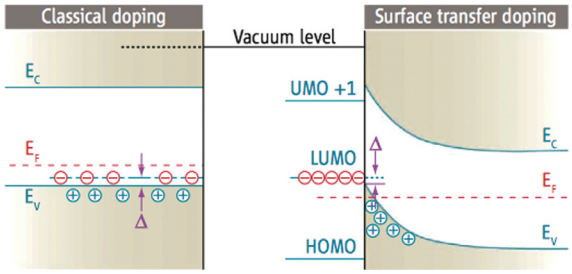

Figure 1. Differences between the classical doping and surface transfer doping. This band diagram illustrates classical *p*-type doping (left) and *p*-type surface transfer doping (right), using the energy of an electron in free space as a reference (vacuum level). Reprinted with permission from [16], J. Ristein, *Science-New York Then Washington* 313, 5790 **(2006)**. © 2006, American Association for the Advancement of Science.

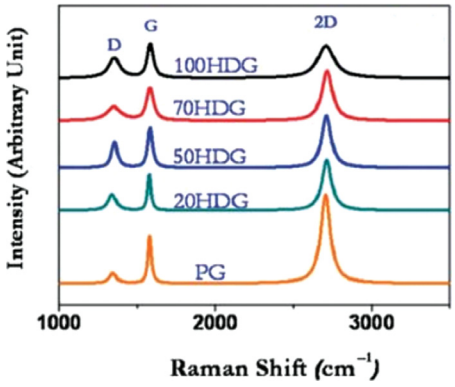

Figure 2. Raman spectra of large scale CVD-graphene doped with different concentrations of nitric acid. The comparative spectra depict the characteristic *D*, *G* and 2*D* Raman bands of pristine and nitric acid treated graphene. Reprinted with permission from [23], S. Das, et al., *J. Mater. Chem.* 22, 38 **(2012).** © 2012, Royal Society of Chemistry.

unoccupied molecular orbitals for electrons (UMOs) and, if the lowest unoccupied molecular orbitals (LUMO) is close to the valance band maximum, electrons are transferred from valance band energy level. If the highest occupied molecular orbitals (HOMO) is close to the valance band maximum, electrons are transferred to the valance band energy level. In the surface charge transfer, electrons and holes are localized on the surface and establish an electrostatic potential. Thus, these charges are confined in a perpendicular direction but make them free to move parallel to the surface.

2.1.1. Acid Treatment

This kind of surface transfer doping is generally studied by using wet chemical doping methods such as H_2SO_4, HCl, HNO_3, etc.[17–20] Among these, nitric acid (HNO_3) is widely used as a *p*-type doping chemical for graphitic materials to improve the charge transfer and conductivity of the carbon-based structures.[21–23] Furthermore, the graphene treated with a HNO_3 solution can control the charge carrier density, band gap, and work function.

In the case of Das et al.[23] to observe the effect of HNO_3 on graphene doping, pristine graphene on glass was dip casted in HNO_3 solutions of 20, 50, 70 and 100%, which addressed as 20, 50, 70, and 100HDG, respectively. Figure 2 shows the Raman spectra of the pristine and HNO_3 doped graphene. As shown in the figure, *D*-band (1342 cm^{-1}) was increased with increasing HNO_3 concentration indicating that the electronic structure of graphene is altered by HNO_3 acid treatments. The authors believed that the alteration of the graphene electronic structure occurred possibly due to the functional bond formation of $C{=}O^-$, $C(O)OH^-$, and NO_3^- with carbon atoms through sp^2–sp^3 hybridization.[23] In order to confirm the *p*-type doping effect of graphene by using HNO_3, ultraviolet photoelectron spectroscopy (UPS) is used as shown in Figure 3(a) and, by using UPS, the band gap and work function of the doped graphene were measured.[23] As illustrated in Figure 3(b), the work function of doped graphene was modified from 4.52 to 5.31 eV due to the hybridization. Due to the Fermi level shift by the work function modification, the characteristic of graphene turned into *p*-type with increased hole concentration.

Figure 3(c) shows another example of graphene doping using a HNO_3 solution. As shown in the figure, the sheet resistance values for the graphene consisted of various numbers of graphene layers were decreased after a HNO_3 doping.[24] That is, the sheet resistance of a roll-to-roll transferred pristine graphene sample was ~280 Ω/sq with 97.4% transmittance, but, after dipping in a 63% HNO_3 solution for 5 min, the sheet resistance of graphene was reduced to ~125 Ω/sq.

2.1.2. Metal Chloride Treatment

Similar results were also found for the graphene doping with metal chlorides.[25–28] Metals with a high work function including Au, Ir, Mo, Os, Pd, etc. have more than 4.98 eV compared to 4.6 eV of pristine graphene.[29] Metal ions in metal chlorides have positive charges. These charges take electrons from graphene due to negative Gibbs free energy and turn into zero charges.[28] Thus, metal chloride materials could be used as *p*-type dopants on graphene to increase its work function.

Figures 4(a) and (b) show the change of sheet resistance and work function as a function of metal chloride *p*-dopants as studied by Kwon et al.[28] The degree of change in the sheet resistance as a function of *p*-dopants is depicted in the inset of (a). The sheet resistance of pristine graphene was reduced differently depending on different metal chlorides, and for $AuCl_3$, a solution composed of 20 mM concentration showed up to 55% reduction of sheet resistance. The work function of graphene was also varied not only with different metal chloride doping but also with the doping concentration. Figure 4(c) shows a model of metal chlorides accepting charges from other materials to reduce Gibbs free energy.[30]

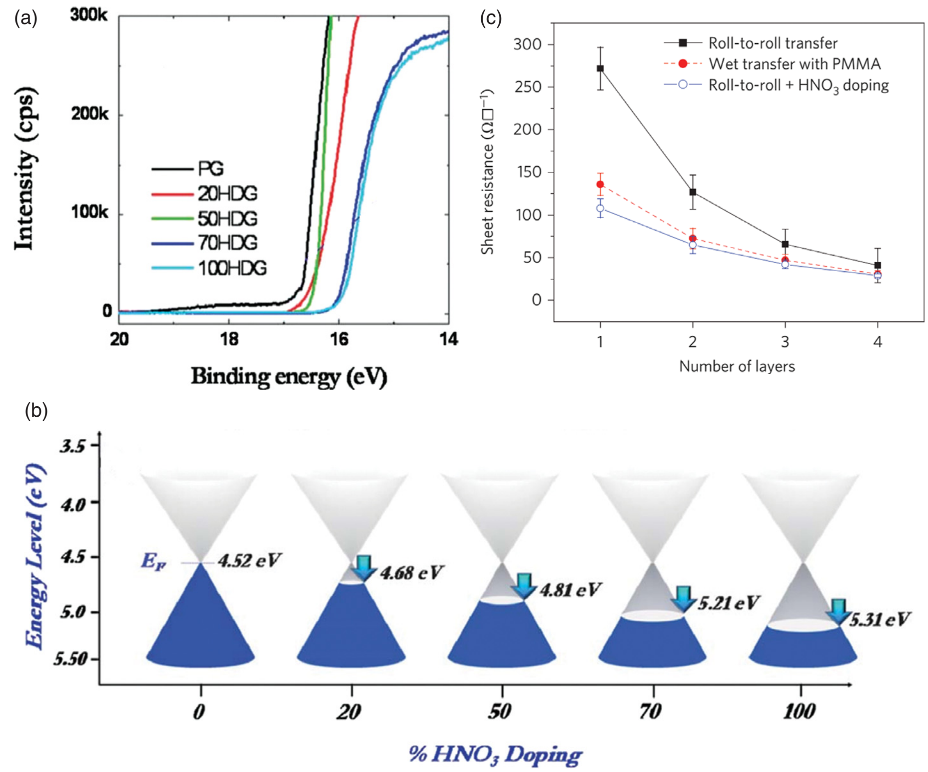

Figure 3. (a) Ultraviolet photoelectron spectroscopy of pristine and HNO_3 doped graphene electrodes under various concentrations (20 to 100%) which depicts the shift in binding energy due to HNO_3 doping. (b) Schematic representation of Fermi level shift in graphene under different concentrations of HNO_3 doping. (a) and (b) Reprinted with permission from [23], S. Das, et al., *J. Mater. Chem.* 22, 38 **(2012)**. © 2012, Royal Society of Chemistry. (c) Sheet resistances of transferred graphene films using a roll-to-roll (R2R) dry-transfer method combined with thermal release tapes and a PMMA-assisted wet-transfer method. Reprinted with permission from [24], S. Bae, et al., *Nat. Nanotechnol.* 5, 8 **(2010)**. © 2010, Nature Publishing Group.

2.1.3. Organic Material Treatment

Even though metal chloride complexes are well known *p*-dopants, metal clusters could reduce optical transmittance of graphene. Therefore, in addition to metal chloride solutions, solutions with organic doping materials such as *N*-phenyl-bis(trifluoromethane sulfonyl)imide (PTFSI), silver bis(trifluoromethane sulfonyl) imide (STFSI), Bis(trifluoromethane sulfonyl) amine, etc. have been studied (their chemical structures are shown in Fig. 5(a)).[31–35] Some of the results on the change of sheet resistance and optical transmittance after the wet doping with organic dopants are shown in Figures 5(b) and (c), respectively. Among these organic dopants, bis(trifluoromethanesulfonyl)amide, so-called TFSA is a well-known *p*-type dopant that has high stability and a remarkable sheet resistance reduction effect.[32] The investigation showed that TFSA could decrease sheet resistance around 70% while the transparency is decreased by only 3% even in the atmosphere.

In order to make *n*-type graphene, a solution containing organic materials (aromatic molecules) such as 1,5-naphthalenediamine ($Na–NH_2$), 9,10-dimethylanthracene ($An–CH_3$), 9,10-dibromoanthracene (An–Br), and tetrasodium 1,3,6,8-pyrenetetrasulfonic acid (TPA), hydrazine (N_2H_4; generally used to reduce graphene oxide), etc. have been used (some of the structures of these aromatic molecules are shown in Fig. 6(a)).[31–35] In Figure 6(b), by using a hydrazine monohydrate solution (N_2H_4–H_2O), the difference between the hydrazine treated graphene film and pristine graphene was demonstrated by Lee et al. by using Raman spectra.[33] As shown in the figure, the 2D peak position of the hydrazine doped graphene was located at 2679 cm^{-1} which is higher than that of pristine 2D peak (2664 cm^{-1}). The movement of 2D peak to higher position for the *n*-type doping was previously confirmed by Dong et al.[35] In general, when graphene is doped *n*-type by surface transfer doping, it is known that *G* peak tends to downshift while *G* peak upshifts when doped with *p*-type by surface transfer doping. The downshifts of *G* peak from 1581 to 1577 cm^{-1} shown in Figure 6(b) also appears to indicate that the graphene is *n*-type doped by hydrazine. Therefore, by observing the change of the peak position, it was confirmed that hydrazine affects graphene to get *n*-type characteristic. Interestingly, the authors also found that hydrazine treatment appeared to decrease I_D/I_G value from 0.35 to 0.25, which means the decrease of defects. Dirac points of hydrazine doped graphene are plotted in Figure 6(c) as a function of hydrazine concentration.

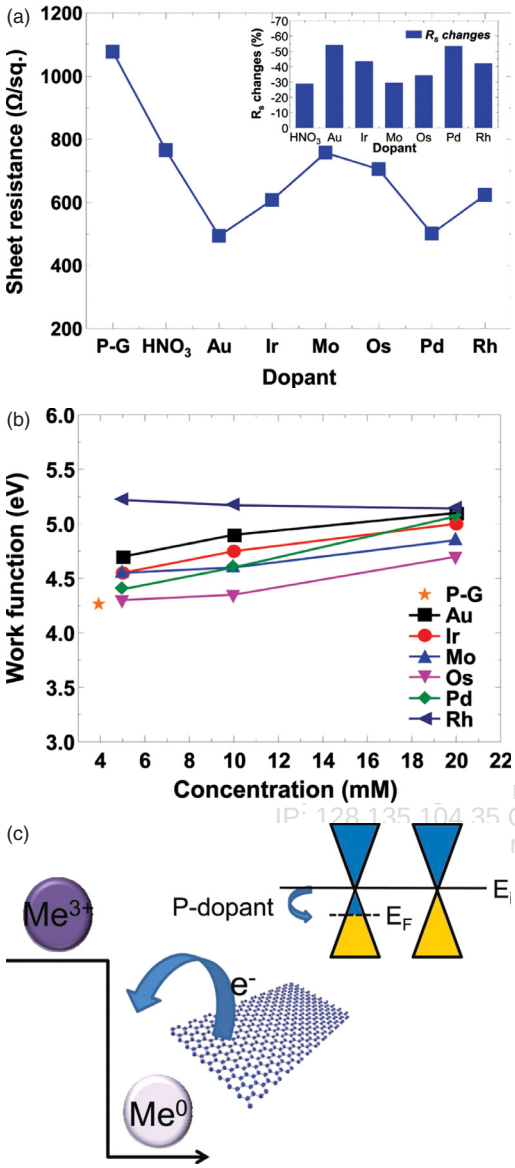

Figure 4. (a) Sheet resistance of PG and doped graphene sheets using metal chlorides. The degree of change in the sheet resistance as a function of *p*-dopants is depicted in the inset of (a). (b) Work function variation as a function of each *p*-dopant with different metal chloride concentration. (c) Schematic of the mechanism for graphene doping by metal chloride. Reprinted with permission from [28], K. C. Kwon, et al., *Adv. Funct. Mater.* 22, 22 **(2012)**. © 2012, Wiley-VCH.

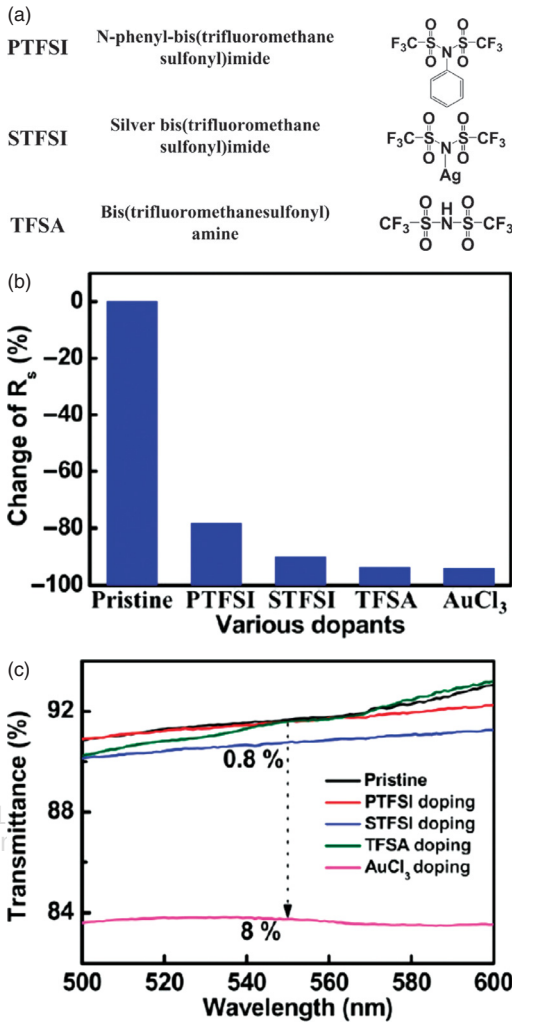

Figure 5. (a) Chemical structures of the various *p*-type graphene dopants and their nomenclature. (b) Sheet resistance of PG and doped graphene sheets using organic dopants. The data are compared with doping with $AuCl_3$. (c) The transmittance for the pristine CNT and PTFSI-doped, STFSI-doped, TFSA-doped, and $AuCl_3$-doped CNT on quartz substrate. Reprinted with permission from [31], S. M. Kim, et al., *ACS Nano* 4, 11 **(2010)**. © 2010, American Chemical Society.

Hydrazine solution effectively modulated its Dirac point and produced *n*-type graphene when the concentration was varied from 0.05 to 100%.

2.2. Dry Doping

In addition to wet doping, graphene can be doped by dry doping methods. Dry doping method could be divided into the electrostatic field doping method, evaporation method, thermal treatment method, plasma doping method, etc.

2.2.1. Electrostatic Field Doping Method

For the control of tunable bandgap, some researchers have investigated the electrical doping method, which is carried out by changing the electric field applied perpendicularly to the sample. This technique can also control the precise doping and provide direct evidence of a widely tunable bandgap.[36–38] Generally, when applying a gate voltage (V_G), an electrostatic potential difference between the graphene and the gate electrode will be created, and the addition of charge carriers by the electric field will lead to

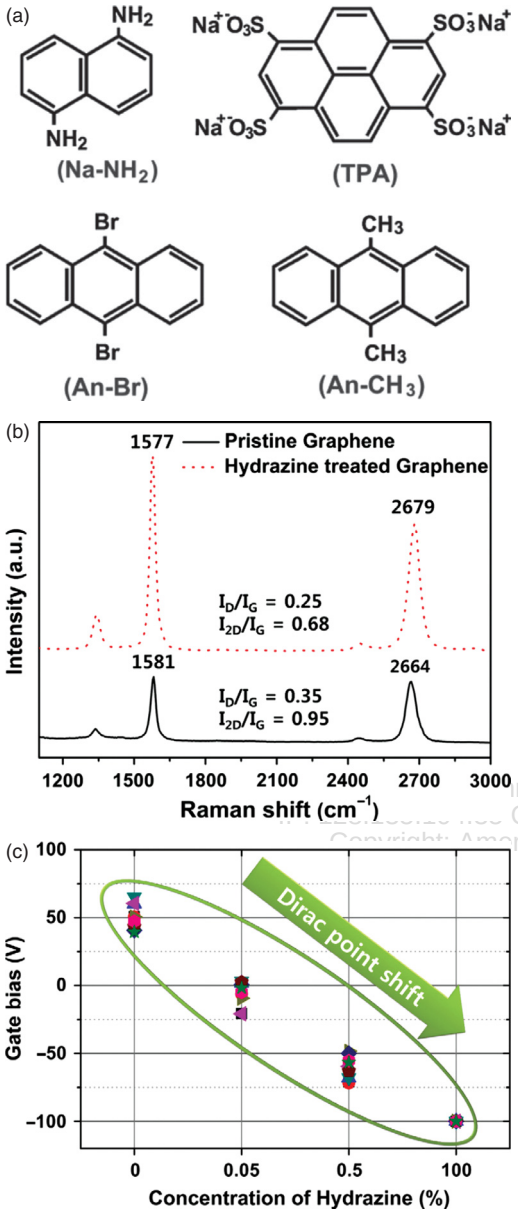

Figure 6. (a) Chemical structures of the aromatic molecules of Na–NH_2, An–Br, An–CH_3, and TPA used as dopants. Reprinted with permission from [35], X. Dong, et al., *Small* 5, 12 (**2009**). © 2009, Wiley-VCH. (b) Raman spectra of pristine and hydrazine treated graphene films. (c) Dirac points of field effect transistors (FETs) as a function of hydrazine concentration. (b) and (c) Reprinted with permission from [33], I. Lee, et al., *Org. Electron.* 14, 1586 (**2013**). © 2013, Elsevier Science.

a shift in the Fermi level (E_F), thus causing modifications of the band structures in the graphene materials.[39]

Zhang et al. demonstrated a gate-controlled, continuously tunable bandgap up to 250 meV by using a dual-gate bilayer graphene field-effect transistor (FET) shown in Figure 7(a).[40] By changing top and bottom gate voltages, one could independently control the electronic band gap

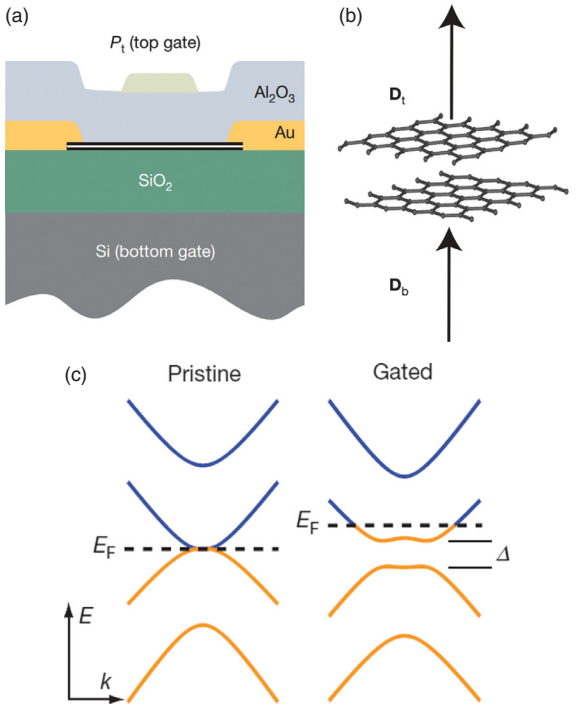

Figure 7. Dual-gated bilayer graphene. (a) Illustration of a cross-sectional side view of the gated device. (b) Sketch showing how gating of the bilayer induces top (D_t) and bottom (D_b) electrical displacement fields. (c) Left, the electronic structure of a pristine bilayer has zero bandgap. (k denotes the wavevector.) Right, upon gating, the displacement fields induces a non-zero bandgap (Δ) and a shift of the Fermi level energy E_F. Reprinted with permission from [40], Y. B. Zhang, et al., *Nature* 459, 820 (**2009**). © 2009, Nature Publishing Group.

and carrier doping concentration. Upon electrical gating, the top and bottom electrical displacement fields caused by top and bottom gate voltages, D_t and D_b in Figure 7(b), produce two effects (Fig. 7(c)): The difference of the two, $dD = D_b - D_t$ leads to a net carrier doping, that is, a shift of the Fermi energy (E_F). The average of the two, $(D_b + D_t)/2$ breaks the inversion symmetry of the bilayer and generates a non-zero bandgap of Δ.[37, 40–42] And, Williams et al. reported that the p-type and n-type carrier density in graphene can be tuned by controlling of the gate voltages.[43]

Although the electrostatic field doping method has abundant merits and excellent results, this method has limitation that cannot be applied to a single layer graphene.[13, 44, 45] Thus, for the bandgap engineering of single graphene, other techniques are neeeded.

2.2.2. Evaporation Method

Graphene can be doped by depositing a thin film of charge transfer material on the graphene surface using thermal evaporation. Figure 8 shows the doping mechanism by the charge transfer of electron from the graphene (p-type) or to the graphene (n-type) by depositing alkali carbonates or transition metal oxides, respectively using thermal

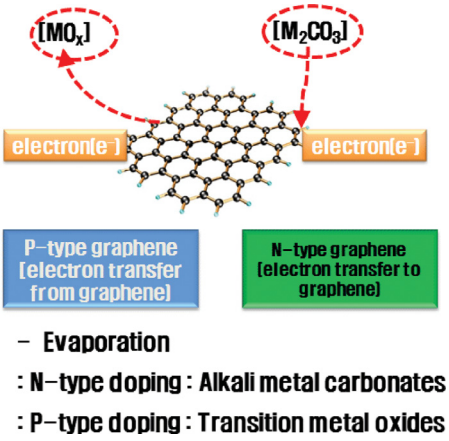

Figure 8. Graphene doping by evaporating surface charge transfer materials.

evaporation. *P*-type doping of graphene can be obtained by deposition of metal oxides such as MoO_3, ReO_3, etc. And *n*-type doping can be obtained by deposition of alkali metal carbonates such as Rb_2CO_3, Cs_2CO_3, etc.

P-type doping can be also obtained by deposition of materials with high electron affinity such as bismuth, antimony, and gold as mentioned in the metal chloride treatment section. However, most of these surface transfer dopants have limited thermal and chemical stability in air, therefore, it is known that these materials are incompatible with thermal processes which may be required for most graphene-based electronic devices. Chen et al.[46] and Xie et al.[47] deposited MoO_3 thin film on the epitaxial graphene (E_G) grown on SiC and the results showed that the large work function difference between the E_G (4.0∼4.3 eV) and MoO_3 (∼6.8 eV) facilitates electron transfer from EG to the MoO_3 thin film. This made hole accumulation in the EG layer with a hole density of about 1.0×10^{13} cm^{-2}, and placed the Fermi level 0.38 eV below the Dirac point.

2.2.3. Thermal Treatment Method

Generally, the doping by thermal treatment means the graphene doping at high temperature (> 800 °C) by the substitutional reaction of carbon atom with dopant atom. In the case of pristine graphene, due to the stable and perfect honeycomb structure, and it is difficult to introduce other dopants into the graphene structure and control the graphene properties even at high temperatures.[48,49] For that reason, an ion irradiation technique has been investigated to increase the reactivity of graphene with dopants by breaking carbon bonds in the graphene structure. Ion irradiation techniques have been previoulsy used for doping of graphite and carbon nanotube (CNT), but for graphene, mostly defect, surface charge, and electronic structure after the ion irradiation has been investigated.[50–54]

Controllable *n*-doping technique through irradiation and postannealing on graphene was introduced by Guo et al.[48]

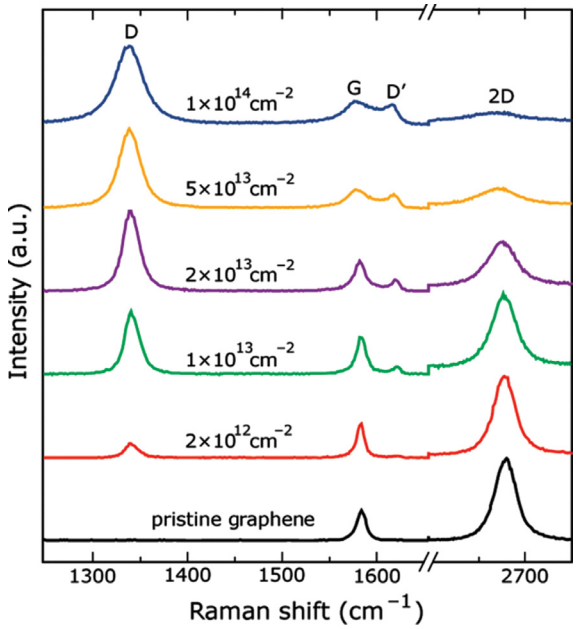

Figure 9. Raman spectra for various fluences of N^+-ions implanted into the same graphene sample. Reprinted with permission from [56], Y.-C. Lin, et al., *Appl. Phys. Lett.* 96, 133110 (**2010**). © 2010, America Chemical Society.

As shown in Figure 9, the Raman spectra of graphene indicate that the disorder increases with the increase of the 30 keV N^+ ion irradiation fluence. After the irradiation, postannealing at 1100 °C for 30 s was carried out in N_2 environment (top figure in Fig. 10) and NH_3 environment (bottom figure in Fig. 10), respectively, and the surface composition was measured using Auger Electron Spectroscopy (AES). In the case of postannealing in N_2, no N signal in graphene was detected and most of the defects from the irradiation were estimated to be vacancy defects.[53,55] However, for the annealing in NH_3, N signal locating at ∼400 eV was detected indicating *N*-doping in graphene. Figure 11 shows the atomic configuration and corresponding schematic band structures of the graphene before and after the substitutional doping of nitrogen atom by thermal treatment after the ion irradiation. The two dimensional honeycomb atomic configuration and zero-gap band structure of the pristine graphene is shown in Figure 11(a).[56–58] After the N^+ ion irradiation, the defects are induced as shown in Figure 11(b) without doping and NH_3 decomposes into atomic N, which can combine with the defect sites of the graphene as displayed in Figure 11(c) to substitutionally replace the carbon sites in the graphene honycomb structure.[58]

Generally, the nitrogen content in the *N*-doped graphene synthesized by this method is known to be relatively low. Geng et al. reported that the highest nitrogen content was 2.8 at.% at 900 °C.[49] The low doping level may be attributed to two reasons: one is the insufficient defect number in the high quality graphene, and the other is the

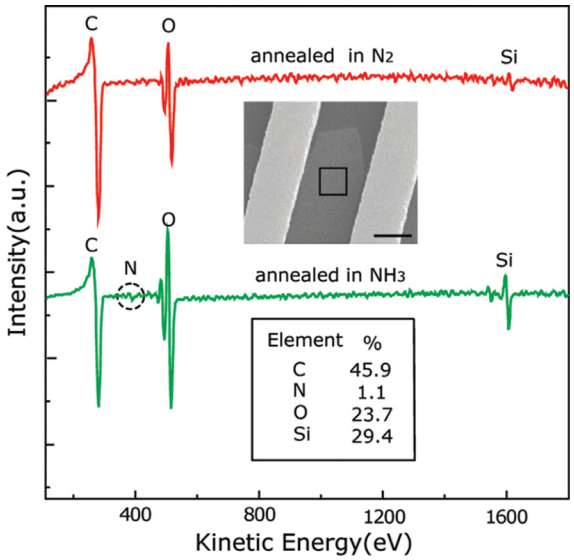

Figure 10. AES data of the graphene annealed in N_2 (red) and in NH_3 (green) at 1100 °C for 30 s, respectively. Reprinted with permission from [56], Y.-C. Lin, et al., *Appl. Phys. Lett.* 96, 133110 (**2010**). © 2010, America Chemical Society.

high annealing temperature, which will break the C—N bonds in the *N*-doped graphene.[48] For the effective control of doping level and electronic properties of graphene, changing the doping parameters, such as dopant species, energy, temperature and irradiation dose should be tuned and optimized.

2.2.4. Plasma Doping

Besides the methods mentined above, plasma treatment can also be used to control electrical properties of graphene through controlling of reaction with graphene and dopant. Many approaches for functionalization by plasma treatment have shown numerous outcomes ranging from *p*-type or *n*-type doping to the widening of its bandgap close to that of an insulator.[56,59–63] Generally, plasma treatment can partly replace carbon atoms in graphene by dopant atoms or can attach dopant atoms to the carbon atoms after breaking the sp^2 carbon bonding; therefore, this method has been applied to synthesize doped-CNTs for a long time.[64–66] Recently, it has been reported that doped-graphene could be prepared from graphene by exposing it to the doping gas plasma.[67–69]

For *p*-type doping, Chen et al. showed that, by using CF_4 or CHF_3 plasma, *p*-doped graphene could be obtained.[70] Raman spectra of the graphene after the CHF_3 or CF_4 plasma treatment (5 W, 5 Pa, 5 sccm) for 10 s in Figure 12 show that the intensity ratio of $I(2D)/I(G)$ is significantly decreased after the plasma treatment because of the attachment of functional fluorine groups to the graphene carbon atoms, that is, the fluorination of the graphene. The attachment of the functional groups changes the hybridization of graphene carbon atoms from sp^2 to

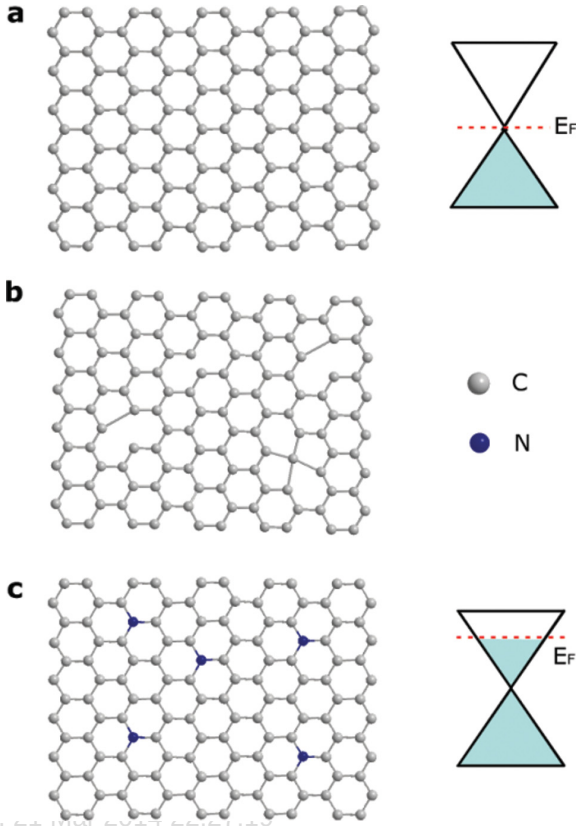

Figure 11. The atomic configuration and corresponding schematic band structures in the graphene sheet. (a) Pristine graphene. (b) The representative vacancy defects of the irradiated graphene. (c) The graphene annealed in NH_3 after irradiation. The doped graphene is formed by substituting some C atoms with N atoms. Reprinted with permission from [56], Y.-C. Lin, et al., *Appl. Phys. Lett.* 96, 133110 (**2010**). © 2010, America Chemical Society.

sp^3 and it disrupts the symmetry.[71–73] Stronger *D*, *D*′ (1620 cm^{-1}) and $D+G$ (2920 cm^{-1}) peaks for the monolayer graphene compared to bilayer and trilayer graphene after the fluorination show that the monolayer graphene is more reactive than the bilayer and trilayer graphene, that is, the monolayer graphene is more fluorinated compared to bilayer and trilayer graphene.

The decrease of the intensity ratio $I(2D)/I(G)$ is also an indication of doping or the presence of charged impurities.[73] The upshifts of the *G* and 2*D* frequencies indicate the *p*-type doping. (In general, for electrical doped graphene or substitutionally doped graphene not by surface transfer doping as shown in the organic matrerial treatment section, *G* band tends to upshift for both *n*-type doping and *p*-type doping.) As shown in Figure 13(a) obtained from the Raman data of the monolayer graphene in Figure 12, the upshifts of those frequencies for CF_4 plasma treated graphene are larger than those of CHF_3 plasma treated graphene, which means that CF_4 plasma treatment causes a higher magnitude of doping to monolayer graphene

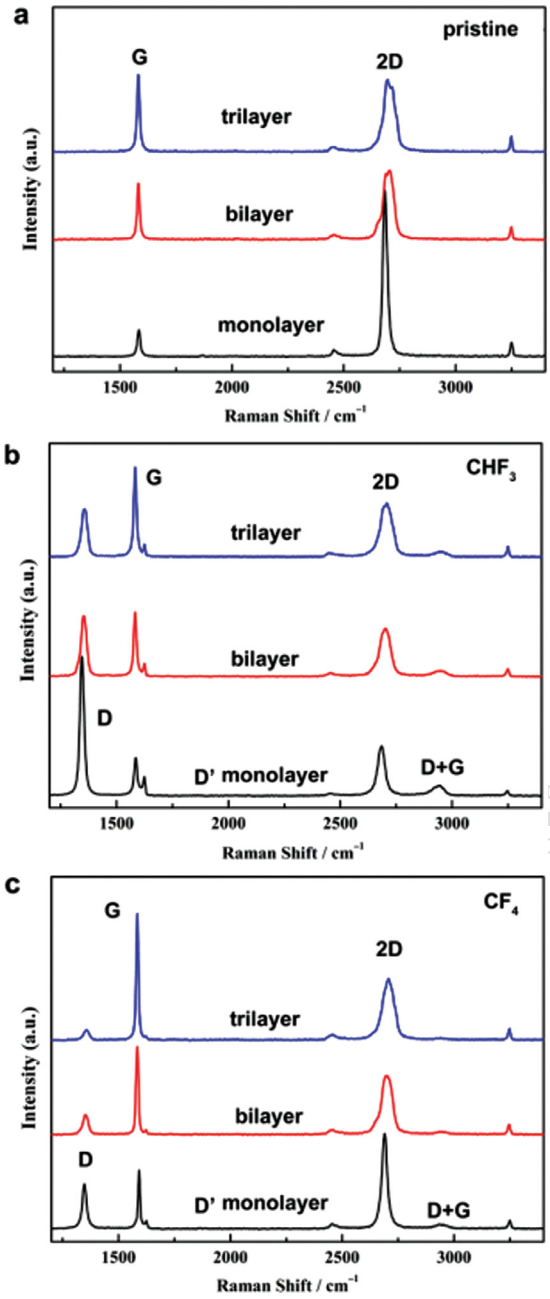

Figure 12. Comparison of the Raman spectra before and after plasma treatment for monolayer, bilayer and trilayer graphene. (a) Raman spectra of pristine graphene. (b) Raman spectra of graphene fluorinated by CHF_3 plasma for 10 s. (c) Raman spectra of graphene fluorinated by CF_4 plasma for 10 s. The plasma treatments are under the same reaction conditions (5 W, 5 Pa, 5 sccm). Reprinted with permission from [70], M. Chen, et al., *Nanotechnology* 23, 115706 **(2012)**. © 2012, IOP publishing.

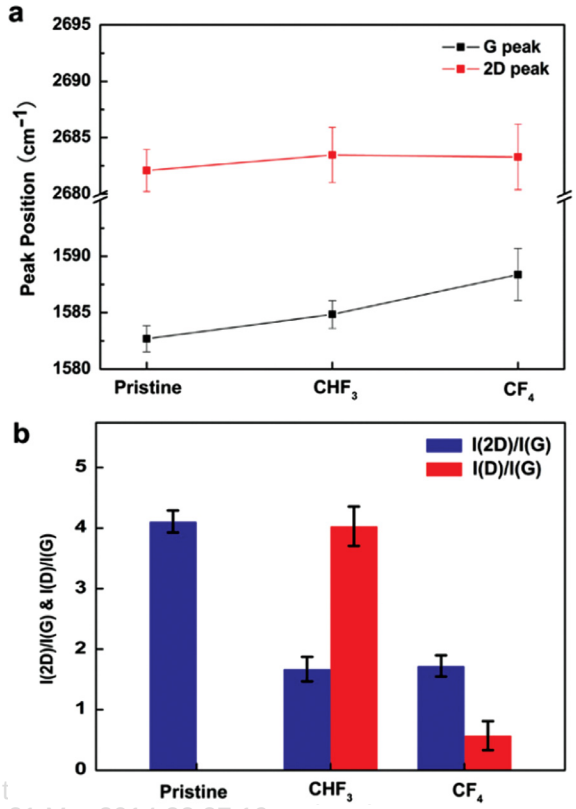

Figure 13. (a) Raman peak positions of the G and $2D$ bands of pristine and plasma treated monolayer graphene. (b) Raman intensity ratios of $I(2D)/I(G)$ and $I(D)/I(G)$ of pristine and plasma treated monolayer graphene. The plasma treatments are under the same conditions (5 W, 5 Pa, 5 sccm, 10 s). Reprinted with permission from [70], M. Chen, et al., *Nanotechnology* 23, 115706 **(2012)**. © 2012, IOP publishing.

compared to CHF_3 plasma treatment in the same experimental conditions.[70] The intensity ratio of $I(D)/I(G)$ is another important parameter and it shows not only the degree of chemical functionalization but also the degree of the vacancies or grain boundaries caused by the high energy active species, that is, a degree of graphene defects. As shown in Figure 13(b), for CHF_3 plasma treated monolayer graphene, a larger $I(D)/I(G)$ while having a smaller $I(2D)/I(G)$ indicates that D peak intensity is basically due to the lattice defects while having a lower magnitude of p-doping. By contrast, CF_4 plasma treated monolayer graphene which has a smaller $I(D)/I(G)$ while having a larger $I(2D)/I(G)$ indicates the lower magnitude of lattice defects and a higher magnitude of p-doping. Therefore, CF_4 plasma is more appropriate for p-type graphene doping.[70, 74, 75]

For the reduction of defects during the plasma treatment, other approaches have been investigated. Dai et al. showed that F and H containing plasma reactions can increase defects and disorder rapidly during plasma fluorination and hydrogenation of graphene, respectively, as shown in Figure 14.[56, 74–76] Cl_2 plasma, however, showed the slowest increase of disorder over the reaction time compared to F and H containing plasma. By using Cl_2 plasma for graphene doping instead of CF_4 or H_2 plasmas, they

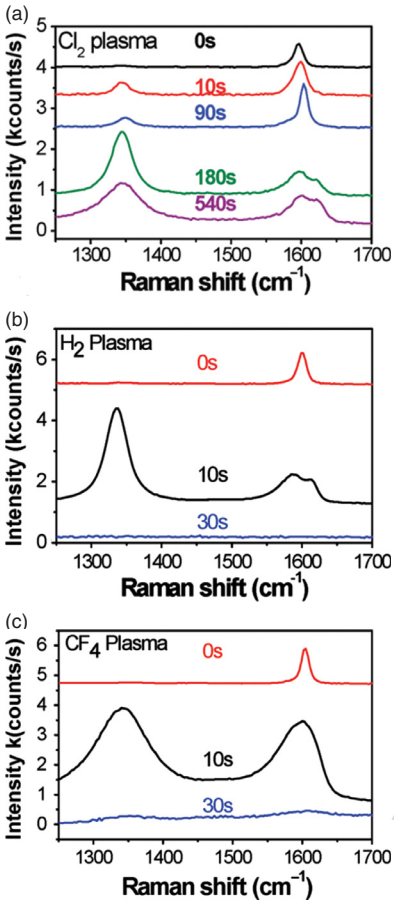

Figure 14. Raman spectra of graphene sheets after plasma treatments of varying time using (a) Cl_2, (b) H_2, and (c) CF_4 plasmas. Reprinted with permission from [76], J. Wu, et al., *J. Am. Chem. Soc.* 133, 19668 (**2011**). © 2011, American Chemical Society.

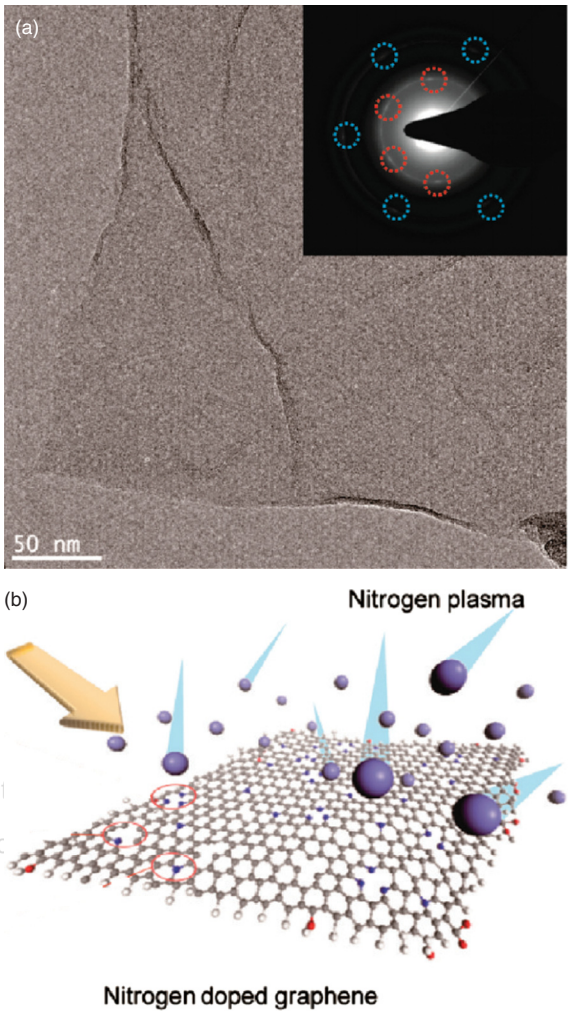

Figure 15. Nitrogen-doped graphene by the plasma treatment. (a) A high-resolution TEM image for the NG (*N* doped Graphene) indicates that the intrinsic layered structure is preserved during the plasma process. Selected area electron diffraction pattern for the NG exhibits diffracted spots (denoted with dotted circles around) in a hexagon position, which is reflective of the preservation of the original honeycomb-like atomic structure of graphene. (b) A schematic illustration of the plasma doping process. By the plasma process with physical momentum, nitrogen atoms replace the existing carbon atoms. Reprinted with permission from [77], H. M. Jeong, et al., *Nano Lett.* 11, 2472 (**2011**). © 2011, American Chemical Society.

obtained the decrease of the sheet resistance of graphene of about 20%.[76]

For the *n*-type doping of graphene, nitrogen and NH_3 plasma have been used as an efficient approach for simple, tunable, and fast preparation of nitrogen-doped graphene (NG). In fact, nitrogen doping in graphene plays a critical role in regulating the electronic properties of carbon materials because nitrogen doping easily controls local electronic structures and thus improves the device performance in various applications.[56, 76, 77] Figure 15(a) shows that a transmission electron microscope (TEM) NG image as well as a selected area electron diffraction (SAED) pattern, and indicate that the original layered structure and honeycomb-like atomic structure of graphene remain unmodified during the plasma processes. Figure 15(b) shows the schematic illustration of the nitrogen plasma doping process, and where nitrogen atoms are expected to replace carbon atoms in the original graphene sheets.[56, 76, 77]

Even though the most of the original graphene honeycomb structure is maintained during the plasma treatment, the graphene surface is generally damaged by ion bombardment during the doping processes by excessively breaking the carbon bonds and by bonding of carbon atoms with unwanted species in the plasma. Therefore, to obtain an effective doping effect, etc. without damaging the graphene surface, that is, for the better control of electrical properties of doped graphene, the plasma variables need to be carefully controlled during the plasma treatment.

3. APPLICATIONS

3.1. Flexible Electronics

High transmittance (over 90%), low sheet resistance (less than 100 Ω/sq), and high Young's modulus are required to fabricate display devices such as organic light-emitting diodes (OLEDs), touch screen displays, *e*-paper, etc. Indium Tin Oxide (ITO) is one of the most widely used transparent conductive materials but it is a ceramic material which is brittle and prone to cracking, therefore, it is limited as a flexible electrode. It has been found that graphene is a suitable and promising material as a transparent conductive film (TCF) due to its high optical transmittance and flexibility except for electrical requirement because the graphenes prepared by CVD growth or graphene flakes prepared by chemical/mechanical exfoliation tend to show high sheet resistances due to the defects in the graphene. For example, the optical transmittance of single CVD graphene layer is 97.7%.[78] However, the sheet resistance of the single CVD graphene layer (> 280 Ω/sq) is much higher than that of ITO (< 30 Ω/sq).[79] Fortunately, the quality of CVD graphene has been improved every year and many researchers have fabricated CVD graphene based OLED by using doping and tuning the work function.[80–82] Graphene has important advantages like flexibility, mechanical strength, high optical transparency, and chemical stability. If contact resistance and sheet resistance performance of the graphene are improved, graphene could probably be used dominantly for flexible electronics.

3.2. Field-Effect Transistor (FET)

It is widely considered that graphene might have an opportunity to replace Si based FET. Because of ultra-fast mobility (on SiO_2 substrate: $\sim 17{,}000$ $cm^2/V \cdot s$, on BN substrate: $\sim 60{,}000$ $cm^2/V \cdot s$, suspended: $\sim 230{,}000$ $cm^2/V \cdot s$)[83–86] many researchers have studied graphene as a gate material for a FET. But it has been discovered that graphene has no band gap critical to transistors that allows it to be turned on and off. Doping, electrostatic field tuning, nanoribbon formation, etc. have been roughly studied as promising ways of opening the band gap. For doping, substitutional heteroatom doping[87–89] and chemical doping modification can be used to open the bandgap and to tune the Fermi level in addition to the electrostatic field tuning by changing gate voltage value to tune the Fermi level of graphene as discussed in the electrostatic field doping method section.

Even for these efforts, due to the low energy band gap of graphene, a graphene based transistor still shows a high leakage current even in off-state. Overcoming such drawback is required to replace Si technology.

3.3. Energy Storage

The conventional cathode materials for energy storage can be modified though doping to enhance conductivity and other electrochemical properties. Carbon additives such as carbon black, carbon coatings, and carbon nanotubes have recently shown remarkable results as conducting additives for the cathode materials. However, in the case of those carbon additives, only a small contact area reacts with active materials and contributes to the electrical conductivity. Graphene is a well-known material with a very high surface/mass ratio in addition to the high theoretical electron conductivity.

Bak et al.[90] have produced a $LiMn_2O_4$ battery combined with graphene sheets and this battery exhibited 137 mA h g^{-1} at 1 C rate superior to nanocrystalline $LiMn_2O_4$ (97 mA h g^{-1} at 1 C rate).[91] Also, the graphene-based supercapacitor fabricated by Liu et al.[92] showed 85.6 Wh/kg, which exceeds (21.4–42.8 Wh/kg) a modern nickel metal hybrid battery. A combination with graphene sheets as electron conducting additive material appears to provide the technology for the next-generation lithium-ion batteries.[93–96] Especially, by doping the graphene, the conductivity of the graphene is increased and it can improve the storage efficiency even further.

3.4. Supercapacitor

The capacity of supercapacitor is proportional to the electrode surface area. The electrochemically active surface attracts ions and charges/discharges ions in seconds. The electric double layer capacitor (EDLC)[97–99] and psuedocapacitor[100,101] have been described as the supercapacitor. The graphene is a suitable electrode material as the super capacitor because of large surface area, good thermal stability, and high electrical conductivity. These properties have shown promising properties as the electrodes for supercapacitor. Especially, by using *n*-doped graphene as the electrode materials, four times larger capacitances (~ 280 $F/g_{electrode}$) have been produced including excellent cycle life (> 200,000), high power capability, and compatibility.[92] And furthermore, graphene with other activated carbons such as CNT is expected to make synergetic effects on supercapacitors.

3.5. Electrochemical Sensors

Graphene based electrochemical sensors such as enzyme biosensors, DNA biosensors, and heavy metal ion sensors have been developed because of its excellent electrochemical bevaviors.[102–107] On the basis of high electrocatalytic activity, graphene has shown a high performance in the enzyme and electrochemical detection of small biomolecules. Also, graphene has exhibited an efficient performance as a heavy metal ion sensor. The electron-transfer-rate constant of the glucose oxidase (GOD) on graphene is 2.83 ± 0.18 s^{-1}, much higher than that reported for CNT, provides fast electron transfer to enzyme and high enzyme loading (1.12×10^{-9} mol/cm^2).[108] And a high electrocatalytic activity of graphene toward H_2O_2 also showed an enhanced performance for detecting H_2O_2. These advantages increased the sensitivity of

graphene-based biosensors.[109] These characteristics can be also improved by doping the graphene due to the increase of the conductivity and chemical selectivity. Further understating of graphene for electroanalysis and electrocatalysis is expected to promote applications to various sensors.

4. CONCLUSION

In this review, we discussed the various wet and dry doping methods of graphene. The graphene is doped by surface charge transfer after the adsorption of dopants on the graphene surface, by substitutionally replacing carbon atom sites in the graphene structure, or by the application of electric field vertically on the graphene surface for the bilayer graphene. For the surface charge transfer mechanism, different from conventional doping obtained for the substitution of carbon atom sites by dopants, when an electron is transferred from the dopant to the graphene, n-type graphene is obtained; and when an electron is transferred from the graphene to the dopant, p-type graphene is obtained. It is clear that the electronic and other electrical properties could be tailored by controlling the doping parameters such as dopant species, concentration, and, especially, by using appropriate doping methods. In addition, because the doping mechanisms are different among various doping methods, it could be possible to increase the doping efficiency even further by combining different doping methods such as combining an acid treatment with a plasma treatment, etc. In the case of plasma doping, the control of the doping concentration without forming defects and disorder of the graphene structure by the ion bombardment is necessary for the better control of electrical properties of the plasma doped graphene. When these factors are controlled more carefully, it is believed that other fascinating properties and phenomena of graphene will be unveiled in the near future.

Acknowledgments: This research was supported by Nanomaterial Technology Development Program through the National Research Foundation of Korea (NRF) funded by the Ministry of Education, Science and Technology (2012035324). And this work was also supported by the Industrial Strategic technology development program (10041926, Development of high density plasma technologies for thin film deposition of nanoscale semiconductor and flexible display processing) funded by the Ministry of Knowledge Economy (MKE, Korea).

References and Notes

1. F. Miao, S. Wijeratne, Y. Zhang, U. C. Coskun, W. Bao, and C. N. Lau, *Science* 317, 5844 (**2007**).
2. S. V. Morozov, K. S. Novoselov, M. I. Katsnelson, F. Schedin, L. A. Ponomarenko, D. Jiang, and A. K. Geim, *Phys. Rev. Lett.* 97, 1 (**2006**).
3. A. K. Geim, and K. S. Novoselov, *Nat. Mater.* 6, 3 (**2007**).
4. A. A. Balandin, S. Ghosh, W. Bao, I. Calizo, D. Teweldebrhan, F. Miao, and C. N. Lau, *Nano Lett.* 8, 3 (**2008**).
5. J. Lee, D. Yoon, and H. Cheong, *Nano Lett.* 12, 9 (**2012**).
6. C. Lee, X. Wei, J. W. Kysar, and J. Hone, *Science* 321, 5887 (**2008**).
7. F. Withers, S. Russo, M. Dubois, and M. F. Craciun, *Nanoscale Res. Lett.* 6, 1 (**2011**).
8. X. Li, Y. Zhu, W. Cai, M. Borysiak, B. Han, D. Chen, R. D. Piner, L. Colombo, and R. S. Ruoff, *Nano Lett.* 9, 12 (**2009**).
9. J. Krupka and W. Strupinski, *Appl. Phys. Lett.* 96, 8 (**2010**).
10. P. Lambin, H. Amara, F. Ducastelle, and L. Henrard, *Phys. Rev. B* 86, 4 (**2012**).
11. R. Lv, Q. Li, A. R. Botello-Méndez, T. Hayashi, B. Wang, A. Berkdemir, Q. Hao, A. L. Elías, R. Cruz-Silva, and H. R. Gutiérrez, *Sci. Rep.* 2, 586 (**2012**).
12. D. Wei, Y. Liu, Y. Wang, H. Zhang, L. Huang, and G. Yu, *Nano Lett.* 9, 5 (**2009**).
13. A. Das, S. Pisana, B. Chakraborty, S. Piscanec, S. Saha, U. Waghmare, K. Novoselov, H. Krishnamurthy, A. Geim, and A. Ferrari, *Nat. Nanotechnol.* 3, 4 (**2008**).
14. J. E. Santos, N. M. Peres, dos Santos, J. M. B. Lopes, and A. H. C. Neto, *Phys. Rev. B* 84, 8 (**2011**).
15. H. Medina, Y. Lin, D. Obergfell, and P. Chiu, *Adv. Funct. Mater.* 21, 14 (**2011**).
16. J. Ristein, *Science-New York Then Washington* 313, 5790 (**2006**).
17. W. J. Zhao, P. H. Tan, J. Zhang, and J. Liu, *Phys. Rev. B* 82, 245423 (**2010**).
18. V. M. Gun'ko, V. V. Turov, R. L. Whitby, G. P. Prykhod'ko, A. V. Turov, and S. V. Mikhalovsky, *Carbon* 57, 191 (**2013**).
19. E. Bouleghlimat, P. R. Davies, R. J. Davies, R. Howarth, J. Kulhavy, and D. J. Morgan, *Carbon* 61, 124 (**2013**).
20. N. A. Cordero and J. A. Alonso, *Nanotechnology* 18, 48 (**2007**).
21. W. Zhou, J. Vavro, N. M. Nemes, J. E. Fischer, F. Borondics, K. Kamaras, and D. Tanner, *Phys. Rev. B* 71, 20 (**2005**).
22. A. Kasry, M. A. Kuroda, G. J. Martyna, G. S. Tulevski, and A. A. Bol, *ACS Nano* 4, 7 (**2010**).
23. S. Das, P. Sudhagar, E. Ito, D. Lee, S. Nagarajan, S. Y. Lee, Y. S. Kang, and W. Choi, *J. Mater. Chem.* 22, 38 (**2012**).
24. S. Bae, H. Kim, Y. Lee, X. Xu, J. Park, Y. Zheng, J. Balakrishnan, T. Lei, H. R. Kim, Y. I. Song, Y. J. Kim, K. S. Kim, B. Özyilmaz, J. H. Ahn, B. H. Lee, and S. Iijima, *Nat. Nanotechnol.* 5, 8 (**2010**).
25. D. H. Shin, J. M. Kim, C. W. Jang, J. H. Kim, S. Kim, and S. Choi, *J. Appl. Phys.* 113, 6 (**2013**).
26. K. C. Kwon, B. J. Kim, J. Lee, and S. Y. Kim, *J. Mater. Chem.C* 1, 13 (**2013**).
27. K. K. Kim, A. Reina, Y. Shi, H. Park, L. Li, Y. H. Lee, and J. Kong, *Nanotechnology* 21, 28 (**2010**).
28. K. C. Kwon, K. S. Choi, and S. Y. Kim, *Adv. Funct. Mater*. 22, 22 (**2012**).
29. T. Takahashi, H. Tokailin, and T. Sagawa, *Physical Review B* 32, 12 (**1985**).
30. S. Y. Kim, K. Hong, K. Kim, H. K. Yu, W. K. Kim, and J. L. Lee, *J. Appl. Phys*. 103, 076101 (**2008**).
31. S. M. Kim, Y. W. Jo, K. K. Kim, D. L. Duong, H. Shin, J. H. Han, J. Choi, J. Kong, and Y. H. Lee, *ACS Nano* 4, 11 (**2010**).
32. S. Tongay, K. Berke, M. Lemaitre, Z. Nasrollahi, D. Tanner, A. Hebard, and B. Appleton, *Nanotechnology* 22, 42 (**2011**).
33. I. Lee, H. Park, J. Park, J. Lee, W. Jung, H. Yu, S. Kim, G. Kim, and J. Park, *Org. Electron.*14, 1586 (**2013**).
34. P. Wei, N. Liu, H. R. Lee, E. Adijanto, L. Ci, B. D. Naab, J. Q. Zhong, J. Park, W. Chen, and Y. Cui, *Nano Lett.* 13, 5 (**2013**).
35. X. Dong, D. Fu, W. Fang, Y. Shi, P. Chen, and L. Li, *Small* 5, 12 (**2009**).
36. T. Ohta, A. Bostwick, T. Seyller, K. Horn, and E. Rotenberg, *Science* 313, 5789 (**2006**).
37. E. V. Castro, K. Novoselov, S. Morozov, N. Peres, J. L. Dos Santos, J. Nilsson, F. Guinea, A. Geim, and A. C. Neto, *Phys. Rev. Lett.* 99, 21 (**2007**).
38. S. Zhou, G. Gweon, A. Fedorov, P. First, W. De Heer, D. Lee, F. Guinea, A. C. Neto, and A. Lanzara, *Nat. Mater.* 6, 10 (**2007**).

39. K. F. Mak, C. H. Lui, J. Shan, and T. F. Heinz, *Phys. Rev. Lett.* 102, 25 (**2009**).
40. Y. B. Zhang, T. T. Tang, C. Girit, Z. Hao, M. C. Martin, and A. Zettl, *Nature* 459, 820 (**2009**).
41. H. K. Min, B. Sahu, S. K. Banerjee, and A. H. MacDonald, *Phys. Rev.* 75, 155115 (**2007**).
42. X. Liu, J. B. Oostinga, A. F. Morpurgo, and L. M. K. Vandersypen, *Phys. Rev*. 80, 121407 (**2009**).
43. J. R. Williams, T. Low, M. S. Lundstrom, and C. M. Marcus, *Nat. Nanotechnol.* 10, 1038 (**2011**).
44. K. S. Novoselov, A. K. Geim, S. V. Morozov, D. Jiang, Y. Zhang, S. V. Dubonos, I. V. Grigorieva, and A. A. Firsov, *Science* 306, 666 (**2004**).
45. A. Avetisyan, B. Partoens, and F. Peeters, *Physical Review B* 79, 3 (**2009**).
46. Z. Chen, I. Santoso, R. Wang, L. F. Xie, H. Y. Mao, H. Huang, Y. Z. Wang, X. Y. Gao, Z. K. Chen, D. Ma, A. T. Wee, and W. Chen, *Appl. Phys. Lett.* 96, 21 (**2010**).
47. L. Xie, X. Wang, H. Mao, R. Wang, M. Ding, Y. Wang, B. Ozyilmaz, K. P. Loh, A. T. Wee, and W. Chen, *Appl. Phys. Lett.* 99, 1 (**2011**).
48. B. Guo, Q. Liu, E. Chen, H. Zhu, L. Fang, and J. R. Gong, *Nano Lett.* 10, 4975 (**2010**).
49. D. Geng, Y. Chen, Y. Chen, Y. Li, R. Li, X. Sun, S. Ye, and S. Knights, *Energ. Environ. Sci.* 4, 760 (**2011**).
50. F. Xu, M. Minniti, C. Giallombardo, A. Cupolillo, P. Barone, A. Oliva, and L. Papagno, *Surf. Sci.* 601, 2819 (**2007**).
51. F. Xu, M. Minniti, P. Barone, A. Sindona, A. Bonanno, and A. Oliva, *Carbon* 46, 1489 (**2008**).
52. B. S. Elman, M. S.Dresselhaus, G. Dresselhaus, E. W. Maby, and H. Mazurek, *Phys. Rev.* 24, 1027 (**1981**).
53. L. Tapaszto', G. Dobrik, P. Nemes-Incze, G. Vertesy, P. Lambin, and L. P. Biro', *Phys. Rev.* 78, 233407 (**2008**).

54. E. Stolyarova, K. T. Rim, S. M. Ryu, J. Maultzsch, P. Kim, L. E. Brus, T. F. Heinz, M. S. Hybertsen, and G. W. Flynn, *Proc. Natl. Acad. Sci.* 104, 9209 (**2007**).
55. L. Tapasztó, P. Nemes-Incze, Z. Osváth, A. Darabont, P. Lambin, and L. P. Biró, *Phys. Rev.* 74, 235422 (**2006**).
56. Y.-C. Lin, C.-Y. Lin, and P.-W. Chiu, *Appl. Phys. Lett.* 96, 133110 (**2010**).
57. Q.-H. Yang, P.-X. Hou, M. Unno, S. Yamauchi, R. Saito, and T. Kyotani, *Nano Lett*. 5, 2465 (**2005**).
58. J. Szczytkoa, P. Juszyńskia, L. Teligaa, A. Stonertb, R. Ratajczakb, A. Kormanb, and A. Twardowskia, *Acta Phys. Pol.* 114, 1387 (**2008**).
59. W. Chen, S. Chen, D. C. Qi, X. Y.Gao, and A. T. S. Wee, *J. Am. Chem. Soc.* 129, 10418 (**2007**).
60. X. Wang, X. Li, L. Zhang, Y. Yoon, P. K. Weber, H. Wang, J. Guo, and H. Dai, *Science* 324, 768 (**2009**).
61. Y. H. Lu, R. Q. Wu, L. Shen, M. Yang, Z. D. Sha, Y. Q. Cai, P. M. He, and Y. P. Feng, *Appl. Phys. Lett.* 94 122111 (**2009**).
62. J. T. Robinson, J. S. Burgess, C. E. Junkermeier, S. C. Badescu, T. L. Reinecke, F. K. Perkins, M. K. Zalalutdniov, J. W. Baldwin, J. C. Culbertson, P. E. Sheehan, and E. S. Snow, *Nano Lett.* 10, 3001 (**2010**).
63. B. Li, L. Zhou, D. Wu, H. Peng, K. Yan, Y. Zhou, and Z. Liu, *ACS Nano* 5, 5957 (**2011**).
64. D. Golberg, Y. Bando, L. Bourgeois, K. Kurashima, and T. Sato, *Carbon* 38, 2017 (**2000**).
65. C. Morant, J. Andrey, P. Prieto, D. Mendiola, J. M. Sanz, and E. Elizalde, *Phys. Status Sol.* 203, 1069 (**2006**).
66. K. Suenaga, M. P. Johansson, N. Hellgren, E. Broitman, W L. R. Allenberg, C. Colliex, J. E. Sundgren, and L. Hultman, *Chem. Phys. Lett.* 300, 695 (**1999**).
67. R. I. Jafri, N. Rajalakshmi, and S. J. Ramaprabhu, *Mater. Chem.* 20, 7114 (**2010**).
68. Y. Wang, Y. Shao, D. W. Matson, J. Li, and Y. Lin, *ACS Nano* 4, 1790 (**2010**).
69. Y. Shao, S. Zhang, M. H. Engelhard, G. Li, G. Shao, Y. Wang, J. Liu, I. A. Aksay, and Y. Lin, *J. Mater. Chem.* 20, 7491 (**2010**).
70. M. Chen, H. Zhou, C. Qiu, H. Yang, F. Yu, and L. Sun, *Nanotechnology* 23, 115706 (**2012**).
71. D. C. Elias, R. R. Nair, T. M. G. Mohiuddin, S. V. Morozov, P. Blake, M. P. Halsall, A. C. Ferrari, D. W. Boukhvalov, M. I. Katsnelson, A. K. Geim, and K. S. Novoselov, *Science* 323, 610 (**2009**).
72. M. Baraket, S. G. Walton, E. H. Lock, J. T. Robinson, and F. K. Perkins, *Appl. Phys. Lett.* 96, 231501 (**2010**).
73. R. Sharma, J. H. Baik, C. J. Perera, and M. S. Strano, *Nano Lett.* 10, 398 (**2010**).
74. J. Yan, Y. B. Zhang, P. Kim, and Pinczuk, *Phys. Rev. Lett.* 98, 166802 (**2007**).
75. S. Pisana, M. Lazzeri, C. Casiraghi, K. S. Novoselov, A. K. Geim, A. C. Ferrari, and F. Mauri, *Nat. Mater.* 6, 198 (**2007**).
76. J. Wu, L. Xie, Y. Li, H. Wang, Y. Ouyang, J. Guo, and H. Dai, *J. Am. Chem. Soc*. 133, 19668 (**2011**).
77. H. M. Jeong, J. W. Lee, W. H. Shin, Y. J. Choi, H. J. Shin, J. K. Kang, and J. W. Choi, *Nano Lett.*11, 2472 (**2011**).
78. L. Falkovsky, *J. Phys.*: *Conference Series* 129, 012004 (**2008**).
79. K. S. Kim, Y. Zhao, H. Jang, S. Y. Lee, J. M. Kim, K. S. Kim, J. Ahn, P. Kim, J. Choi, and B. H. Hong, *Nature* 457, 7230 (**2009**).
80. T. Han, Y. Lee, M. Choi, S. Woo, S. Bae, B. H. Hong, J. Ahn, and T. Lee, *Nat. Photonics* 6, 2 (**2012**).
81. J. Wu, M. Agrawal, H. A. Becerril, Z. Bao, Z. Liu, Y. Chen, and P. Peumans, *ACS Nano* 4, 1 (**2009**).
82. S. Pang, Y. Hernandez, X. Feng, and K. Müllen, *Adv. Mater.* 23, 25 (**2011**).
83. Y. Zhang, Y. Tan, H. L. Stormer, and P. Kim, *Nature* 438, 7065 (**2005**).
84. X. Hong, K. Zou, and J. Zhu, *Phys. Rev. B* 80, 24 (**2009**).
85. C. Dean, A. Young, I. Meric, C. Lee, L. Wang, S. Sorgenfrei, K. Watanabe, T. Taniguchi, P. Kim, and K. Shepard, *Nature Nanotechnol*. 5, 10 (**2010**).
86. K. I. Bolotin, K. Sikes, Z. Jiang, M. Klima, G. Fudenberg, J. Hone, P. Kim, and H. Stormer, *Solid State Commun*. 146, 9 (**2008**).
87. L. Panchakarla, K. Subrahmanyam, S. Saha, A. Govindaraj, H. Krishnamurthy, U. Waghmare, and C. Rao, *Adv. Mater.* 21, 46 (**2009**).
88. M. Endo, T. Hayashi, S. Hong, T. Enoki, and M. S. Dresselhaus, *J. Appl. Phys*. 90, 11 (**2001**).
89. H. Wang, Q. Wang, Y. Cheng, K. Li, Y. Yao, Q. Zhang, C. Dong, P. Wang, U. Schwingenschlögl, and W. Yang, *Nano Lett.* 12, 1 (**2011**).
90. S. Bak, K. Nam, C. Lee, K. Kim, H. Jung, X. Yang, and K. Kim, *J. Mater. Chem*. 21, 43 (**2011**).
91. W. Tang, X. Wang, Y. Hou, L. Li, H. Sun, Y. Zhu, Y. Bai, Y. Wu, K. Zhu, and T. van Ree, *J. Power Sources* 198, 308 (**2012**).
92. C. Liu, Z. Yu, D. Neff, A. Zhamu, and B. Z. Jang, *Nano Lett.* 10, 12 (**2010**).
93. J. K. Lee, K. B. Smith, C. M. Hayner, and H. H. Kung, *Chem. Commun.* 46, 12 (**2010**).
94. N. Li, G. Liu, C. Zhen, F. Li, L. Zhang, and H. Cheng, *Adv. Func. Mater.* 21, 9 (**2011**).
95. H. Wang, Y. Yang, Y. Liang, J. T. Robinson, Y. Li, A. Jackson, Y. Cui, and H. Dai, *Nano Lett.* 11, 7 (**2011**).
96. H. Xiang, K. Zhang, G. Ji, J. Y. Lee, C. Zou, X. Chen, and J. Wu, *Carbon* 49, 5 (**2011**).
97. Y. Sun, Q. Wu, and G. Shi, *Energy Environmental Sci.* 4, 4 (**2011**).
98. M. Liang, B. Luo, and L. Zhi, *Int. J. Energy Res.* 33, 13 (**2009**).
99. L. Zhang and G. Shi, *J. Phys. Chem. C* 115, 34 (**2011**).
100. H. Wang, H. S. Casalongue, Y. Liang, and H. Dai, *J. Am. Chem. Soc.* 132, 21 (**2010**).

101. M. D. Stoller, S. Park, Y. Zhu, J. An, and R. S. Ruoff, *Nano Lett.* 8, 10 **(2008)**.
102. S. Alwarappan, C. Liu, A. Kumar, and C. Li, *J. Phys. Chem. C* 114, 30 **(2010)**.
103. Q. Zeng, J. Cheng, L. Tang, X. Liu, Y. Liu, J. Li, and J. Jiang, *Adv. Func. Mater.* 20, 19 **(2010)**.
104. L. Wu, H. Chu, W. Koh, and E. Li, *Optics Express* 18, 14 **(2010)**.
105. Y. Bo, H. Yang, Y. Hu, T. Yao, and S. Huang, *Electrochim. Acta* 56, 6 **(2011)**.
106. Y. Bo, W. Wang, J. Qi, and S. Huang, *Analyst* 136, 9 **(2011)**.
107. Z. Tang, H. Wu, J. R. Cort, G. W. Buchko, Y. Zhang, Y. Shao, I. A. Aksay, J. Liu, and Y. Lin, *Small* 6, 11 **(2010)**.
108. M. Zhou, Y. Zhai, and S. Dong, *Anal. Chem.* 81, 14 **(2009)**.
109. X. Kang, J. Wang, H. Wu, I. A. Aksay, J. Liu, and Y. Lin, *Biosens. Bioelectron.* 25, 4 **(2009)**.

Received: 10 August 2013. Accepted: 4 November 2013.